Biosensors and Bioelectronics 79 (2016) 843–849

Contents lists available at ScienceDirect

Biosensors and Bioelectronics

journal homepage: www.elsevier.com/locate/bios

Selective determination of phenols and aromatic amines based on horseradish peroxidase-nanoporous gold co-catalytic strategy

Chao Wu [1], Zhuang Liu [1], Huihui Sun, Xia Wang *, Ping Xu [2]

State Key Laboratory of Microbial Technology, Shandong University, Jinan 250100, PR China

ARTICLE INFO

Article history:
Received 20 October 2015
Received in revised form
19 December 2015
Accepted 10 January 2016
Available online 11 January 2016

Keywords:
Horseradish peroxidase
Nanoporous gold
Biosensor
Phenols
Aromatic amines

ABSTRACT

Aromatic compounds, such as phenols and aromatic amines, are environmental contaminants suspected of posing human health risks. For phenols and aromatic amines reliable detection, promoting selectivity and sensitivity for phenols and aromatic amines is crucial in biosensor design. Here, a biosensor combined the advantages of both enzymatic and nonenzymatic electrochemical sensors is constructed. Nanoporous gold (NPG) is selected as an enzyme carrier for horseradish peroxidase (HRP) biosensor fabrication due to its three-dimension structure with unique properties. It is firstly discovered that NPG can achieve selective oxidation for phenols and aromatic amines. Thus, the electrochemical reaction on the resulting HRP/NPG/GCE bioelectrode is attributed to the co-catalysis of HRP and NPG. For the detection of catechol (Cat), 4-aminophenol (*p*-AP), *o*-phenylenediamine (*o*-PD), and *p*-phenylenediamine (*p*-PD), linear responses are observed in large concentration ranges with high sensitivities and low detection limits. Further, the HRP/NPG/GCE bioelectrode presents strong reproducibility, specificity, selectivity and anti-interference capability in detecting the mixture of phenols and aromatic amines along with a long shelf-life, and the real sea water sample analysis was achieved. These unique properties make the HRP/NPG/GCE bioelectrode an excellent choice for phenols and aromatic amines reliable detection.

1. Introduction

In view of the deteriorating natural environment, the importance of establishing accurate, specific, rapid, and sensitive analytical tools to detect environmental pollutants is increasingly prominent (Rodriguez-Mozaz et al., 2004). Among all the environmental pollutants, aromatic compounds, especially phenols and aromatic amines, had the notoriety because of their strong stability, great harmfulness, and poor biodegradability (Kulys and Vidziunaite, 2003; Mourya et al., 2011). Phenols commonly presented in wastewater from gas works, coking plants, refineries, metallurgical plants, and other industries (Silva et al., 2011). Aromatic amines were the intermediate of dyes, pigments, pesticides, additives, and photographic materials (Mourya et al., 2011; Sax, 1975). Unfortunately, these compounds could be directly released into soil and ground water through industrial effluent, becoming an important environmental pollution indicator for their toxicity to aquatic organisms and long-term damage to aquatic environment (Asthana et al., 2000; Davi and Gnudi., 1999). Besides, reports also announced that phenols and aromatic amines were carcinogenic (Hirose et al., 1993; Matsumoto et al., 2012; Najafi et al., 2014). Therefore, an efficient and simple determination method of phenols and aromatic amines was urgently needed for environmental monitoring.

Compared with traditional methods available for pollutants detection, biosensor has unique advantages such as high selectivity and sensitivity, easy operation, fast response, and continuous on-line detection (Suprun et al., 2004; Karimi-Maleh et al., 2015). As an extensively studied enzyme, horseradish peroxidase (HRP) has been widely used in biosensors for phenols and aromatic amines detection (Çevik et al., 2012; Elyacoubi et al., 2006; Morales et al., 2005). Chekin et al. immobilized HRP on varieties of screen-printed carbon electrodes for phenols monitoring (Chekin et al., 2015). Chen et al. assembled HRP/glucose oxidaze (GOx) bienzyme biosensor due to sugar–lectin biospecific interactions for amperometric determination of phenols and aromatic amines (Chen et al., 2008). In those biosensors, HRP was oxidized by hydrogen peroxide, and then reduced by phenols or aromatic amines as electron donors (Ruzgas et al., 1996). However, none of the existing HRP biosensors had the capability to determine a certain aromatic compound from a group of phenols or aromatic amines, thus the poor selectivity and resolution of those biosensors strongly limited their practical potential. Lei et al. reported a

* Corresponding author.
E-mail address: ghwx@sdu.edu.cn (X. Wang).
[1] These authors contributed equally to this work.
[2] Present address: Key Laboratory of Microbial Metabolism and School of Life Sciences and Biotechnology, Shanghai Jiao Tong University, Shanghai 200240, PR China.

http://dx.doi.org/10.1016/j.bios.2016.01.026
0956-5663/

Boron-doped diamond film electrode that could detect phenol, hydroquinone, and 4-nitrophenol with separated oxidative peaks (Lei et al., 2007). But there were no biosensors achieved selective determination for phenols and aromatic amines so far.

In recent years, various nanomaterials with high sensing performance, intimate enzyme attachment, and effective electron transfer were employed as enzyme immobilization supports and as recognition elements in electrochemical sensors (Karimi-Maleh et al., 2013, 2014). Among that, nanoporous gold (NPG) has attracted great attention in enzyme-based biosensor constructing due to its three-dimensional porous morphology, unique electrochemical catalytic performance as well as good biocompatibility, active surface, and excellent conductivity (Ding et al., 2004; Ding and Chen, 2009; Scanlon et al., 2012; Yan et al., 2012; Zhang and Ding, 2013). According to Liu et al., gold-based nonenzymatic electrode could selectively determine *p*-nitrophenol in the presence of *o*-nitrophenol and *m*-nitrophenol (Liu et al., 2011). Although there were no related reports, we suppose NPG may possess catalytic activity towards phenols and aromatic amines for the analogous redox behavior of phenols and aromatic amines as electron donors. Besides, different compounds may be selectively detected because of their distinct redox states at the NPG/solution interface related to the various position of substituted hydroxyl or amino group. Therefore, NPG might offer high specificity in phenols and aromatic amines detection, while HRP could enhance the catalytic activity as a signal amplification strategy that significantly increasing the sensitivity.

In our previous work, HRP/NPG biocomposites were successfully constructed by assembling HRP onto NPG. And the remarkable catalytic activity of the resulting HRP/NPG biocomposites was achieved (Wang et al., 2011). Based on the assumption of co-catalytic strategy discussed above, this study was aimed at designing and developing a high performance HRP/NPG biosensor for selective determination of phenols and aromatic amines. Due to the excellent and stable performances of the HRP/NPG biocomposites, the HRP/NPG biosensor is expected to exhibit high selectivity and sensitivity in phenols and aromatic amines determination.

2. Experimental

2.1. Chemicals

HRP (Roche11378783 from horse radish, grade II) was purchased from F. Hoffmann-La Roche Ltd. (Basel, Switzerland). Catechol (Cat, analytical grade) was purchased from Tianjin Damao Chemical Reagent Factory (Tianjin, China). 4-Aminophenol (*p*-AP, 97%) was purchased from J&K Scientific Ltd. (Beijing, China). *o*-Phenylenediamine (*o*-PD, chemically pure) was purchased from Sinopharm Chemical Reagent Co., Ltd. (Shanghai, China). *p*-Phenylenediamine (*p*-PD, analytical grade) was purchased from Tianjin Kermel Chemical Reagent Co., Ltd. (Tianjin, China). All other chemicals used are of analytical grade.

The phenols and aromatic amines were dissolved in absolute ethanol to form 10 mM substrate stock solutions. The substrate stock solutions were stored in a refrigerator at 4 °C in the dark.

2.2. Preparation of NPG/GCE electrode

NPG was made by dealloying 12-carat white gold leaves (Au50Ag50 wt%, Sepp Leaf Products, USA) in concentrated HNO_3 at 30 °C for 30 min. After that, NPG was washed with ultrapure water until the pH to 7.0. It was then kept in ultrapure water.

Glassy carbon electrodes (GCEs) were polished with a 0.05 μm alumina slurry on a piece of chamois leather. Before use, the GCEs were cleaned ultrasonically in the mixture of HNO_3 and water mixed in a 1:1 ratio (v/v), and washed with ultrapure water and absolute ethanol, respectively. The GCE was then coated with an NPG leaf in ultrapure water to form NPG/GCE. The NPG/GCE was placed in a vacuum drier for later use.

2.3. HRP immobilization

HRP solution (4 mg mL^{-1}) is freshly prepared by dissolving 4 mg HRP in 800 μL PBS (50 mM, pH 7.0) and 200 μL dimethyl sulfoxide prior to being used. The freshly prepared NPG/GCE was immersed immediately in HRP solution. After 72 h immobilization, the HRP/NPG/GCE bioelectrode was immersed in PBS (50 mM, pH 7.0) and stored in a refrigerator at 4 °C until use.

2.4. Measurement

The morphology of NPG was characterized using a Nova NanoSEM 450 field emission scanning electron microscope (SEM) equipped with an energy-dispersive X-ray spectrometer (EDS).

All electrochemical measurements were performed in a conventional three-electrode cell at room temperature. Cyclic voltammograms (CVs), linear sweep voltammograms (LSVs), and differential pulse voltammograms (DPVs) were measured using a three-electrode conventional cell with a CHI 760D electrochemical workstation (Shanghai Chenhua Apparatus Corporation, China). The modified GCE was used as a working electrode, and a Pt sheet (1 cm × 1 cm) and a saturated calomel electrode (SCE) were used as counter and reference electrodes, respectively. All potentials were referred to the SCE. The electrolyte solutions were deaerated by N_2 bubbling for 10 min prior to electrochemical measurements, and a blanket of N_2 was maintained throughout each experiment.

2.5. Detection of phenols and aromatic amines concentration

10 μL H_2O_2 (30 wt%) was added to 15 mL deaerated PBS (50 mM, pH 8.0) as combined substrate prior detection. Substrate stock solutions were added to this reaction solution in a three-electrode system with the HRP/NPG/GCE bioelectrode as working electrode. During real sea water sample analysis, the sea water sample (200 μL) was added and detected at the same condition using the HRP/NPG/GCE bioelectrode as the working electrode.

3. Results and discussion

3.1. Construction and characterization of HRP/NPG/GCE bioelectrode

In our previous work, HRP/NPG biocomposite was successfully constructed by assembling HRP onto the surface of NPG, and NPG with a pore size of ca. 35 nm was proved to help achieve the maximum stabilization (Wang et al., 2011; Wu et al., 2015). The linkage of NPG and HRP in constructing the HRP/NPG/GCE bioelectrode is depicted in Fig. 1. The samples before (Fig. 1A) and after (Fig. 1B) HRP loading were characterized using SEM. Fig. 1A illustrates an open three-dimensional nanoporous structure, which provides a bridge to link the underlying electrode and the active sites of enzyme in bioelectrode construction (Wang et al., 2011; Qiu et al., 2012; Wu et al., 2014, 2015). Evidently, a smaller pore size and coarser surface morphology of the HRP/NPG biocomposite (Fig. 1B) relative to the bare NPG (Fig. 1A) was confirmed, demonstrating a preferential immobilization of HRP over the ligament site with high radial curvatures. Additionally, dominant elements such as C, N, and O was detected on HRP/NPG biocomposite by an energy-dispersive X-ray spectrometer (EDS) analysis (Fig. 1C), thus providing the primary evidence for a successful HRP immobilization onto NPG.

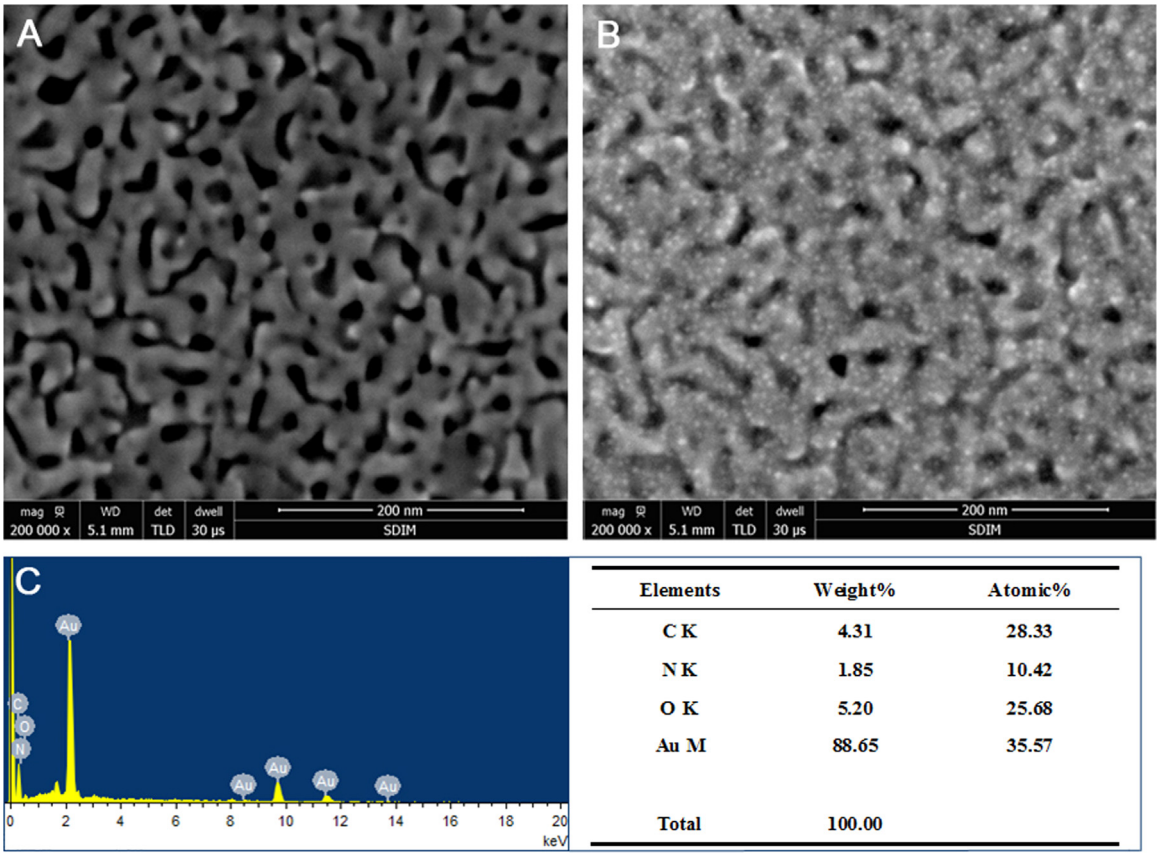

Elements	Weight%	Atomic%
C K	4.31	28.33
N K	1.85	10.42
O K	5.20	25.68
Au M	88.65	35.57
Total	100.00	

Fig. 1. SEM images of NPG with a pore size of 35 nm before (A) and after HRP loading (B); along with the corresponding EDS spectra (C).

3.2. *Electrochemical behavior of HRP/NPG/GCE bioelectrode*

The electrochemical behaviors of NPG/GCE electrode and HRP/NPG/GCE bioelectrode were compared in deaerated PBS (50 mM, pH 7.0) at the scan rate of 50 mV s^{-1}. Apparently, the current response of the HRP/NPG/GCE bioelectrode was lower than that of the NPG/GCE electrode as shown in Fig. 2A. A charge-transfer barrier caused by the insulating character of HRP makes a lower current response after HRP loading, indicating that HRP was successfully assembled into NPG (Zhang et al., 2005; Qiu et al., 2012).

Fig. 2B shows a group of CVs for the HRP/NPG/GCE bioelectrode in deaerated PBS (50 mM, pH 7.0) at different scan rates ranging from 10 mV s^{-1} to 400 mV s^{-1}. It was obvious that the redox peak current density is dependent on the scan rate. As shown in the inset of Fig. 2B, by plotting the peak current density against the square root of scan rate, a perfect linear relationship between the peak current density and the square root of scan rate was obtained. The regression coefficients for cathodic and anodic peak were 0.999 and 0.986, respectively, confirming that the electron transfer process was a diffusion-controlled process (Li et al., 2015).

To confirm the functioning of the HRP/NPG/GCE bioelectrode during the electrocatalytic oxidation of phenols and aromatic amines, the HRP/NPG/GCE bioelectrode and NPG/GCE electrode were compared in deaerated PBS (50 mM, pH 7.0) with the presence of 10 µL H_2O_2 (30 wt%), accompanied with 100 µM *p*-AP (Fig. 2C) and 100 µM *o*-PD (Fig. 2D) respectively, by sweeping the DPV curves. Fig. 2C shows that both NPG/GCE electrode and HRP/NPG/GCE bioelectrode showed electrocatalytic activity during *p*-AP oxidation. According to Liu et al., gold-based nonenzymatic electrode could determine *p*-nitrophenol (Liu et al., 2011). To our knowledge, it was first discovered that NPG could electrocatalytically oxidize none-nitro phenols and aromatic amines. Notably, A higher peak current density of the HRP/NPG/GCE bioelectrode was observed at +0.04 V as compared to that of the NPG/GCE electrode because of the efficient catalysis of HRP, thus indicating a better catalytic activity towards *p*-AP than that of the nonenzymatic NPG/GCE electrode. Besides, both NPG/GCE electrode and HRP/NPG/GCE bioelectrode showed electrocatalytic activity towards *o*-PD as shown in Fig. 2D, and the HRP/NPG/GCE bioelectrode still exhibited better catalytic activity due to the higher peak current density at +0.21 V. Once again, these results indicated that the electrochemically active HRP was successfully immobilized onto NPG. Upon HRP loading, the encapsulated enzyme occupied parts of the active sites of NPG, as evidenced by a slightly decreased current density in Fig. 2A. However, a remarkably enhanced current was observed with the presence of phenols and aromatic amines, indicating that covering HRP on NPG could significantly promote phenols and aromatic amines sensing rather than affecting phenols and aromatic amines oxidizing catalyzed by NPG. Meanwhile, the peak shape of the HRP/NPG/GCE bioelectrode was sharper according to Fig. 2D. Otherwise, the NPG/GCE electrode exhibited peak tailing as shown in Fig. 2C and D. This demonstrated that the assembling of HRP could strengthen the sensing performance of electrode over again. Commonly, the reaction of HRP consists of the oxidation of HRP by H_2O_2, the reduction of intermediate compounds by electron donors (AH_2, phenols or aromatic amines), and the reduction of oxidized electron donors (AH●) by electrode (Ruzgas et al., 1996). As for the HRP/NPG/GCE bioelectrode, the oxidation of AH_2 was catalyzed by both HRP and NPG. In this case, the working principle of the HRP/NPG/GCE bioelectrode during the electrocatalytic oxidation of phenols and aromatic amines could be expressed as follows:

$$2AH_2 + H_2O_2 \xrightarrow[HRP]{} 2AH\bullet + 2H_2O \quad (1)$$

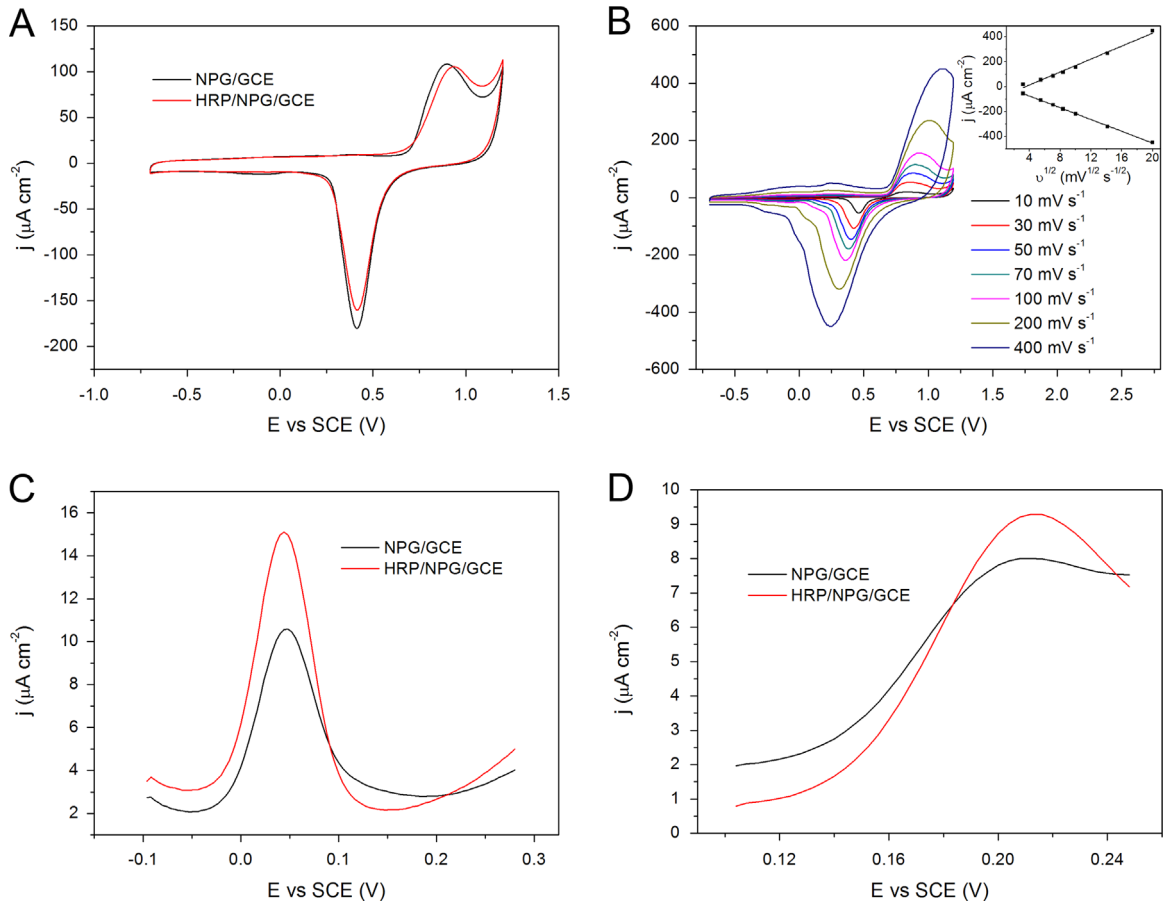

Fig. 2. CVs of NPG/GCE electrode and HRP/NPG/GCE bioelectrode in PBS (50 mM, pH 7.0) (A). CVs of HRP/NPG/GCE bioelectrode at different scan rates ranging from 10 to 400 mV s^{-1} (B); the inset profile shows the peak current density as a function of the square root of scan rate. DPVs of the HRP/NPG/GCE bioelectrode in the presence of 10 μL H_2O_2 (30 wt%) in PBS (50 mM, pH 7.0) with 100 μM *p*-AP (C) or 100 μM *o*-PD (D).

$$AH_2 \xrightarrow[NPG]{} AH\bullet + e^- + H^+ \quad (2)$$

$$AH\bullet + e^- + H^+ \xrightarrow[Electrode]{} AH_2 \quad (3)$$

In this way, the reaction of Eqs. (1) and (2) carried out simultaneously, and AH● produced by both pathways was reduced in the same place as described in Eq. (3). Therefore, the higher current density of the HRP/NPG/GCE bioelectrode shown in Fig. 2C and D could be the result of enhanced electrochemical oxidation signal due to the synergistic effect of HRP and NPG towards phenols and aromatic amines. Based on above results, the electrochemical reaction on the surface of the HRP/NPG/GCE bioelectrode was attributed to the co-catalysis of HRP and NPG, as shown in Scheme 1. Such co-catalytic signal amplification strategy offered a better current response than that of HRP or NPG alone. Therefore, phenols and aromatic amines detection was achieved by detecting the changes of the oxidation peak current density using the HRP/NPG/GCE bioelectrode.

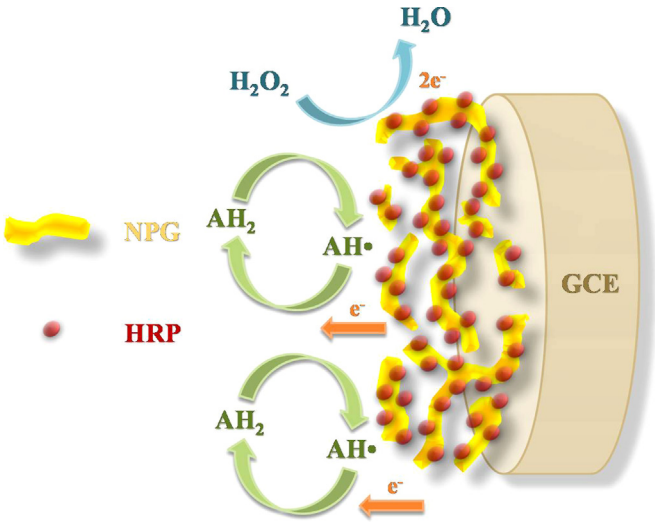

Scheme 1. Electrochemical reaction of HRP/NPG/GCE bioelectrode.

3.3. *Isolating detection of phenols and aromatic amines*

The electrochemical response of the HRP/NPG/GCE bioelectrode was investigated using DPV and LSV technique in deaerated PBS (50 mM, pH 7.0). Successive addition of Cat (Fig. 3A), *p*-AP (Fig. 3B), *o*-PD (Fig. 3C), and *p*-PD (Fig. 3D) as substrates ranging from 0.5 to 200 μM were detected respectively. As shown in Fig. 3, while the substrate concentration increased, the peak current density of the HRP/NPG/GCE bioelectrode also increased proportionately. The peak current density of the HRP/NPG/GCE bioelectrode as a function of concentration showed linear relationships within a certain concentration range, and the linearity, correlation coefficient, sensitivity, and detection limit for four substrates are summarized in Fig. 3E in detail. For the determination of phenols and aromatic amines, the widest linear range of 2–180 μM was achieved against *o*-PD, and the highest sensitivity and the lowest detection limit were respectively calculated to be

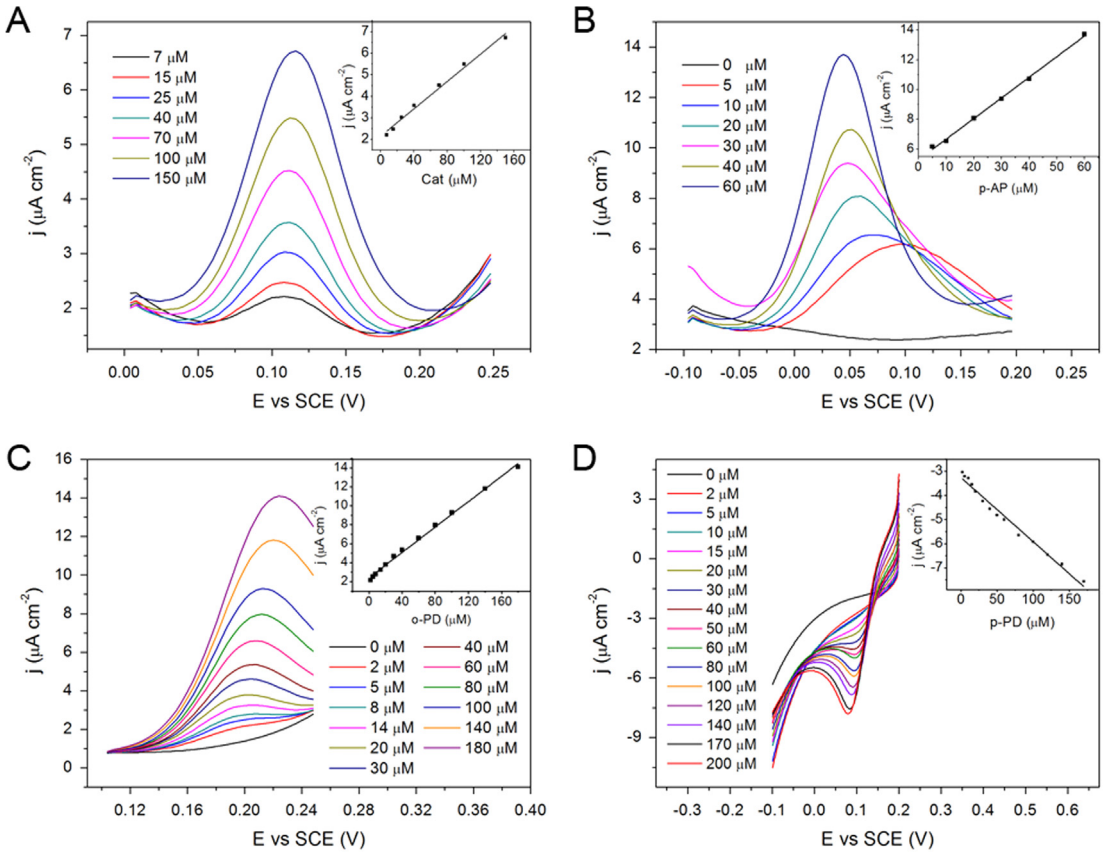

E

Compound	Linear range (μM)	Detection limit (μM)	Sensitivity (μA cm^{-2} mM^{-1})	Peak potential (V)
Catechol	7-150	0.66	31.8	0.12
p-aminophenol	5-60	0.11	187.3	0.04
o-Phenylenediamine	2-180	0.36	67	0.21
p-Phenylenediamine	2-170	0.33	26.5	0.10

Fig. 3. Electrochemical response of the HRP/NPG/GCE bioelectrode as a function of Cat (A), *p*-AP (B), *o*-PD (C), and *p*-PD (D) concentration, the inset profiles showing the calibration curve between the peak current density and the concentration. The performance of the HRP/NPG/GCE bioelectrode in detecting phenols and aromatic amines (E).

0.11 μM and 187.3 μA mM^{-1} cm^{-2} against *p*-AP. These results indicated that the HRP/NPG/GCE bioelectrode possessed larger linear concentration ranges, higher sensitivities, and lower detection limits than most enzymatic or nonenzymatic phenols and aromatic amines sensors, as shown in Table S1 (Supporting Information). Moreover, the peak potential of four substrates evidently varies from each other as listed in Fig. 3E, which provides an ideal possibility for simultaneous and selective detection of the mixture of phenols and aromatic amines.

3.4. Selective detection of the mixture of phenols and aromatic amines

The specificity and selectivity of biosensor is an important characteristic for the applied and specific recognition of the target substrate. Considering the separated peak potential in amperometric detections of phenols and aromatic amines, the specificity and selectivity of the HRP/NPG/GCE bioelectrode was tested by simultaneously and selectively detecting the mixture of phenols and aromatic amines as shown in Fig. 4. During this experiment, the electrochemical response of the HRP/NPG/GCE bioelectrode was investigated using the DPV technique in deaerated PBS (50 mM, pH 7.0) within a potential range from −0.1 V to +0.28 V, which contained the peak potential of those phenols and aromatic amines. To detect the mixture of phenols and aromatic amines, the electrochemical responses of the HRP/NPG/GCE bioelectrode towards 100 μM *p*-AP and 100 μM *o*-PD were measured respectively then simultaneously. As shown in Fig. 4A, the oxidation peaks of *p*-AP and *o*-PD were separated obviously at +0.04 V and +0.18 V, respectively. Notably, when the mixture of *p*-AP and *o*-PD was tested, two oxidation peaks of both *p*-AP and *o*-PD were observed at the same potential (+0.04 V for *p*-AP; +0.18 V for *o*-PD). Meanwhile, the two peak current densities of the mixture were in good agreement with those of *p*-AP or *o*-PD alone, suggesting that simultaneous or separate detection of phenols and aromatic amines was quite feasible.

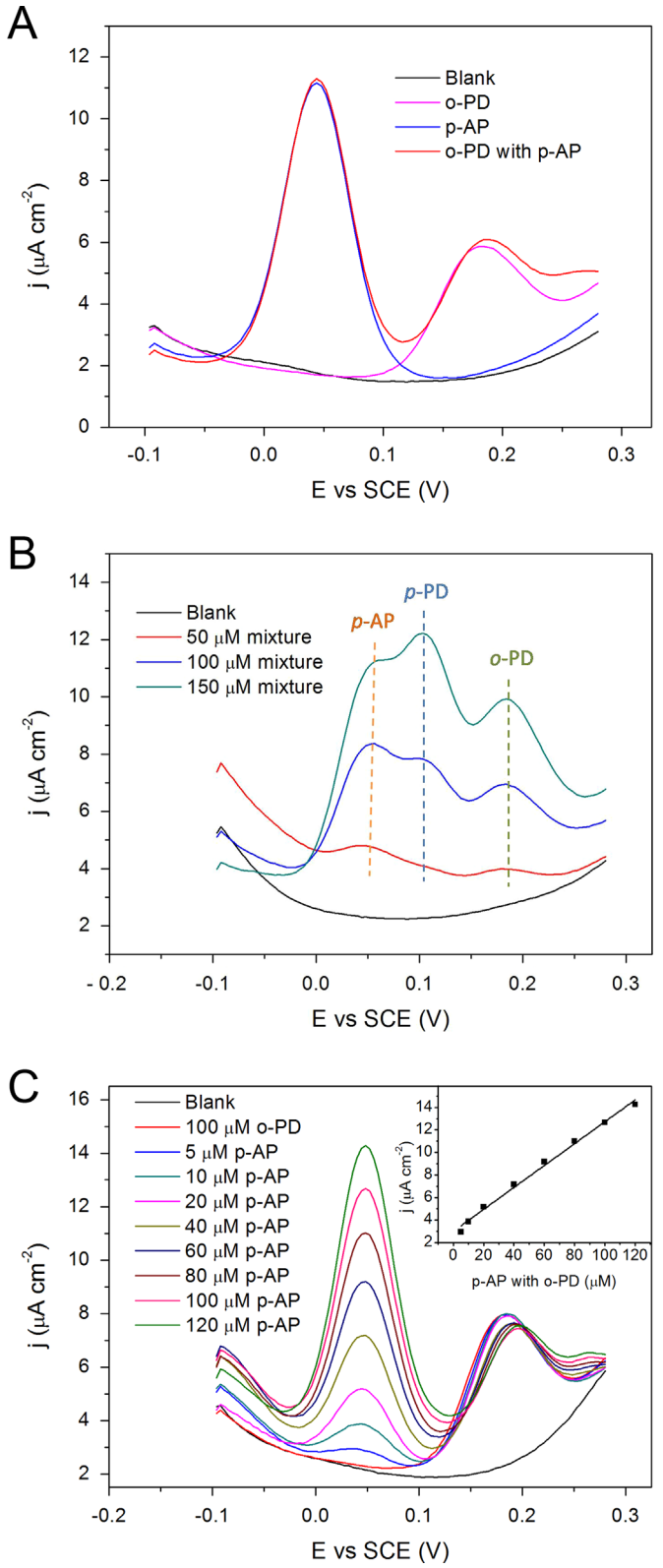

Fig. 4. DPVs of the HRP/NPG/GCE bioelectrode in the presence of 10 μL H_2O_2 (30 wt%) in PBS (50 mM, pH 7.0) with 100 μM *p*-AP, 100 μM *o*-PD, and the mixture of 100 μM *p*-AP and *o*-PD (A) or the mixture of *p*-AP, *p*-PD, and *o*-PD ranging from 50 to 150 μM (B). Electrochemical response of the HRP/NPG/GCE bioelectrode as a function of the *p*-AP concentration (5–120 μM) with the presence of 100 μM *o*-PD (C). The inset profile shows the calibration curve between the peak current density and the concentration.

Further experiment was carried out by evaluating the electrochemical response of the HRP/NPG/GCE bioelectrode towards the multicomponent solution containing *p*-AP, *p*-PD, and *o*-PD. Fig. 4B shows that DPVs of the mixture have three anodic peaks, located at +0.05 V, +0.10 V and +0.18 V, belonging to *p*-AP, *p*-PD, and *o*-PD respectively. As the concentration of mixture raised from 50 to 150 μM, the level of three oxidation peaks increased unequally with a reliable linearity due to the different sensitivity of the HRP/NPG/GCE bioelectrode towards various compounds. The difference of peak potential may be related to the position of substituted hydroxyl or amino group. Because of the different molecular orbital energies and pK_a values, it is possible that different compounds display distinct redox states at the electrode/solution interface (Liu et al., 2011). These results indicated that the appearance of any one compound does not affect the detection of other compounds.

To further confirm the practical performance of the HRP/NPG/GCE bioelectrode in detecting the multicomponent solution, the electrochemical response of the HRP/NPG/GCE bioelectrode was investigated as a function of *p*-AP concentrations (5–120 μM) using DPV technique with the presence of 100 μM *o*-PD in deaerated PBS (50 mM, pH 7.0). As shown in Fig. 4C, while the *p*-AP concentration increased, the oxidation peak current density of the HRP/NPG/GCE bioelectrode also increased at the potential of +0.04 V. Moreover, the peak current densities were all proportional to the *p*-AP concentration in an even larger range (5–120 μM) than in the independent determination of *p*-AP (5–60 μM), with a correlation coefficient of 0.993. A high sensitivity of 97.2 μA mM^{-1} cm^{-2} and a low detection limit of 0.27 μM were also achieved. Furthermore, the peak current densities of *o*-PD at the potential of +0.18 V remained nearly constant when the oxidation peak of *p*-AP rising. During the 9 consecutive measurements, a low relative standard deviation (RSD) of 2.72% for the peak current densities of coexisting 100 μM *o*-PD was achieved, demonstrating that the HRP/NPG/GCE bioelectrode exhibited good reproducibility. Thus, the HRP/NPG/GCE bioelectrode could provide a strong specificity and selectivity during the practical determination of phenols and aromatic amines.

3.5. Anti-interference capability of HRP/NPG/GCE bioelectrode

The anti-interference capability of enzyme electrode is important in specific recognition. The specificity and selectivity of the HRP/NPG/GCE bioelectrode was tested and described as mentioned above. Further examination of anti-interference ability was carried out by adding interferents while simultaneously detecting *p*-AP and *o*-PD. During this experiment, 50 μM *m*-Phenylenediamine (*m*-PD), *o*-Cresol (*o*-CR), and *p*-hydroxybenzoic acid (*p*-HA) were added into the deaerated PBS (50 mM, pH 7.0) containing 50 μM *p*-AP and *o*-PD to evaluate the anti-interference ability of the HRP/NPG/GCE bioelectrode. Fig. 5A shows that after the respective addition of *m*-PD, *o*-CR, and *p*-HA, negligible changes in the current signal were observed in simultaneously detecting *p*-AP and *o*-PD. These results indicated that the presence of interferents barely affected the process of phenols and aromatic amines detection. Thus, the HRP/NPG/GCE bioelectrode showed a strong anti-interference capability during the practical determination of phenols and aromatic amines.

3.6. Stability and reproducibility of HRP/NPG/GCE bioelectrode

Stability is a basic requirement for each biosensor. The HRP/NPG/GCE bioelectrode was preserved in ultrapure water at 4 °C to investigate its stability. After a 32 day storage, the HRP/NPG/GCE bioelectrode retained 98.2% of its initial current response, confirming that the HRP/NPG/GCE bioelectrode presented good

A

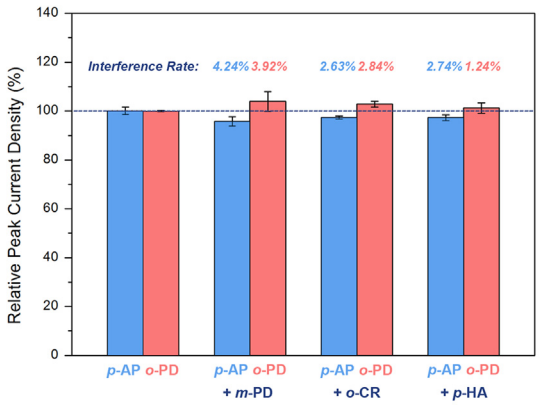

B

Sea water sample	Phenols	Aromatic amines
From Shanghai	21.19 μM *p*-AP	30.46μM *o*-PD
From Cape of Good Hope 1#	-	-
From Cape of Good Hope 2#	-	-

Fig. 5. Effects of interferents on HRP/NPG/GCE bioelectrode (A). Real sea water sample detection with HRP/NPG/GCE bioelectrode (B).

stability because of the good biocompatibility and the rarely inactivating catalytic sites provided by NPG (Ravindra et al., 2004; Sotiropoulou et al., 2005; Hudson et al., 2008; Wang et al., 2011; Wu et al., 2014, 2015). For investigating the reproducibility of the HRP/NPG/GCE bioelectrode, five consecutive measurements were recorded by detecting the current response of the HRP/NPG/GCE bioelectrode in the presence of 40 μM *o*-PD, and the RSD were 0.88%. The considerably low RSD indicated that the HRP/NPG/GCE bioelectrode exhibited good reproducibility.

3.7. Detection of sea water samples

The practical performance of the HRP/NPG/GCE bioelectrode was evaluated by detecting phenols and aromatic amines concentration in actual sea water samples. The sea water samples were collected from the sea water pump of steamer cabin . As to the three samples tested, phenols and aromatic amines were only detected in the sea water sample gathered near Zhoushan Islands, China. A rapid and stable response current density value was acquired at +0.04 V and +0.21 V, suggesting that the sample contained *p*-AP and *o*-PD. By substituting the value into the calibration curve, the concentration of *p*-AP and *o*-PD in this sample was respectively calculated. The obtained results are shown in Fig. 5B. This result demonstrated that the as-prepared biosensor was practical and effective for the determination of phenols and aromatic amines in real water samples.

4. Conclusion

In summary, by encapsulating HRP onto NPG, the fabrication of HRP/NPG/GCE bioelectrode for reliable detection of phenols and aromatic amines was successfully achieved. With a three-dimensional nanoporous structure, NPG provided a good interface between the active sites of enzyme and the underlying electrode. The efficient electrocatalytic oxidation of phenols and aromatic amines on the resulting HRP/NPG/GCE bioelectrode was realized by the co-catalytic signal amplification strategy based on the interaction of HRP and NPG, thus offering excellent sensing performance with high sensitivity, reproducibility, and good stability. Additionally, the reliable selective detection and real sample analysis for phenols and aromatic amines by the HRP/NPG/GCE bioelectrode provide an excellent choice for the practical determination of phenols and aromatic amines.

Acknowledgments

This work was supported by grants from the National Natural Science Foundation of China (21177074 and 31570103), Shandong Science & Technology Fund Planning Project (2014GSF117021), and State Key Laboratory of Microbial Metabolism Fund of Shanghai Jiao Tong University (MMLKF14-07).

Appendix A. Supplementary material

Supplementary data associated with this article can be found in the online version at http://dx.doi.org/10.1016/j.bios.2016.01.026.

References

Asthana, A., Bose, D., Durgbanshia, A., Sanghib, S.K., Kok, W.T., 2000. J. Chromatogr. A 895, 197–203.
Çevik, E., Senel, M., Baykal, A., Abasiyanik, M.F., 2012. Sens. Actuators B 173, 396–405.
Chekin, F., Gorton, L., Tapsobea, I., 2015. Anal. Bioanal. Chem. 407, 439–446.
Chen, Z.C., Xi, F.N., Yang, S.M., Wu, Q., Lin, X.F., 2008. Sens. Actuators B 130, 900–907.
Davi, M.L., Gnudi, F., 1999. Water Res. 14, 3213–3219.
Ding, Y., Kim, Y., Erlebacher, J., 2004. Adv. Mater. 16, 1897–1900.
Ding, Y., Chen, M.W., 2009. MRS Bull. 34, 569–576.
Elyacoubi, A., Zayed, S.I.M., Blankert, B., Kauffmann, J.M., 2006. Electroanalysis 18, 345–350.
Hirose, M., Fukushima, S., Tanaka, H., Asakawa, E., Takahashi, S., Ito, N., 1993. Carcinogenesis 14, 525–529.
Hudson, S., Cooney, J., Magner, E., 2008. Angew. Chem. Int. Ed. 47, 8582–8594.
Lei, Y.Z., Zhao, G.H., Liu, M.C., Xiao, X., Tang, Y.T., Li, D.M., 2007. Electroanalysis 10, 1445–1450.
Li, L.L., Wang, Y.Q., Pan, L.J., Shi, Y., Cheng, W., Shi, Y., Yu, G.H., 2015. Nano Lett. 15, 1146–1151.
Liu, Z.N., Zhang, H.C., Ma, H.Y., Hou, S.F., 2011. Electroanalysis 23, 2851–2861.
Karimi-Maleh, H., Biparva, P., Hatami, M., 2013. Biosens. Bioelectron. 48, 270–275.
Karimi-Maleh, H., Tahernejad-Javazmi, F., Ensafi, A.A., Moradi, R., Mallakpourm, S., Beitollahi, H., 2014. Biosens. Bioelectron. 60, 1–7.
Karimi-Maleh, H., Tahernejad-Javazmi, F., Atar, N., Yola, M.L., Gupta, V.K., Ensafi, A. A., 2015. Ind. Eng. Chem. Res. 54, 3634–3639.
Kulys, J., Vidziunaite, R., 2003. Biosens. Bioelectron. 18, 319–325.
Matsumoto, M., Suzuki, M., Kano, H., Aiso, S., Yamazaki, K., Fukushima, S., 2012. Arch. Toxicol. 86, 791–804.
Morales, M.D., Gonzalez, M.C., Serra, B., Zhang, J.B., Reviejo, A.J., Pingarron, J.M., 2005. Electroanalysis 19, 1780–1788.
Mourya, S.K., Bose, D., Durgbanshi, A., Esteve-Romero, J., Carda-Broch, S., 2011. Anal. Methods 3, 2032–2040.
Najafi, M., Khalilzadeh, M.A., Karimi-Maleh, H., 2014. Food Chem. 158, 125–131.
Qiu, C.C., Wang, X., Liu, X.Y., Hou, S.F., Ma, H.Y., 2012. Electrochim. Acta 47, 140–146.
Ravindra, R., Zhao, S., Gies, H., Winter, R., 2004. J. Am. Chem. Soc. 126, 12224–12225.
Ruzgas, T., Csçregi, E., Emneus, J., Gorton, L., Marko-Varga, G., 1996. Anal. Chim. Acta 330, 123–138.
Rodriguez-Mozaz, S., Maria-Pilar, M., de Lopez, A.M., Barceló, D., 2004. Pure Appl. Chem. 76, 723–752.
Sax, N.I., 1975. Dangerous Propertiesof Industrial Materials, 4th ed.16. Van Nostrand Reinholds Co., NewYork, p. 408.
Scanlon, M., Salaj-Kosla, U., Belochapkine, S., MacAodha, D., Leech, D., Ding, Y., Magner, E., 2012. Langmuir 28, 2251–2261.
Silva, L.M.C., Salgado, A.M., Coelho, M.A.Z., 2011. Environ. Technol. 32, 493–497.
Sotiropoulou, S., Vamvakaki, V., Chaniotakis, N.A., 2005. Biosens. Bioelectron. 20, 1674–1679.
Suprun, E.V., Budnikov, H.C., Evtugyn, G.A., Brainina, Kh.Z., 2004. Bioelectrochemistry 63, 281–284.
Wang, X., Liu, X., Yan, X., Zhao, P., Ding, Y., Xu, P., 2011. PLoS One 6, e24207.
Wu, C., Liu, X., Li, Y., Du, X., Wang, X., Xu, P., 2014. Biosens. Bioelectron. 53, 26–30.
Wu, C., Sun, H., Li, Y., Liu, X., Du, X., Wang, X., Xu, P., 2015. Biosens. Bioelectron. 66, 350–355.
Yan, X., Meng, F., Xie, Y., Liu, J., Ding, Y., 2012. Sci. Rep. 2, 941.
Zhang, S., Wang, N., Niu, Y., Sun, C., 2005. Sens. Actuators B 109, 367–374.
Zhang, X., Ding, Y., 2013. Catal. Sci. Technol. 3, 2862–2868.